Biochimica et Biophysica Acta 1850 (2015) 2283–2292

Contents lists available at ScienceDirect

Biochimica et Biophysica Acta

journal homepage: www.elsevier.com/locate/bbagen

Mode of DNA binding with γ-butyrolactone receptor protein CprB from *Streptomyces coelicolor* revealed by site-specific fluorescence dynamics

Anwesha Biswas [a], Satya Narayan [b], Mamata V. Kallianpur [b], G. Krishnamoorthy [b,*], Ruchi Anand [a,*]

[a] Department of Chemistry, Indian Institute of Technology Bombay, Mumbai, Maharashtra 400076, India
[b] Department of Chemical Sciences, Tata Institute of Fundamental Research, Mumbai, Maharashtra 400005, India

ARTICLE INFO

Article history:
Received 9 April 2015
Received in revised form 16 July 2015
Accepted 12 August 2015
Available online 14 August 2015

Keywords:
2-Aminopurine
γ-Butyrolactone
Anisotropy
Fluorescence lifetime

ABSTRACT

Background: The γ-butyrolactone (GBL) binding transcription factors in *Streptomyces* species are known for their involvement in quorum sensing where they control the expression of various genes initiating secondary metabolic pathways. The structurally characterized member of this family CprB from *Streptomyces coelicolor* had earlier been demonstrated to bind a multitude of sequences containing a specific binding signature. Though structural breakthrough has been obtained for its complex with a consensus DNA sequence there is, however a dearth of information regarding the overall and site specific dynamics of protein–DNA interaction.
Methods: To delineate the effect of CprB on the bound DNA, changes in motional dynamics of the fluorescent probe 2-aminopurine were monitored at three conserved base positions (5th, 12th and 23rd) for two DNA sequences: the consensus and the biologically relevant cognate element, on complex formation.
Results: The changes in lifetime and generalized order parameter revealed a similarity in the binding pattern of the protein to both sequences with greater dynamic restriction at the end positions, 5th and 23rd, as compared to the middle 12th position. Also differences within this pattern demonstrated the influence of even small changes in sequence on protein interactions.
Conclusions: Here the study of motional dynamics was instrumental in establishing a structural footprint for the cognate DNA sequence and explaining the dynamics for the consensus DNA from structural correspondence.
General significance: Motional dynamics can be a powerful tool to efficiently study the mode of DNA binding to proteins that interact differentially with a plethora of DNA sequences, even in the absence of structural breakthrough.

1. Introduction

The system controlling protein expression in a cell relies on a class of proteins known as transcription factors [1–4]. These proteins recognize their cognate DNA via different DNA binding motifs, like the zinc finger [5,6] and helix-turn-helix (HTH) motifs [7–9]. In most cases binding to DNA induces a conformational change that primes them for either transcription repression or activation [2,3]. Many transcription factors are pleiotropic in nature and bind to a multitude of DNA sequences containing conserved elements [10,11]. This allows them to exert a finer level of control over DNA by allowing gradations of expression and at times they also serve as autoregulators of their own expression [12,13]. In *Streptomyces* the onset of secondary metabolic pathways like morphological differentiation, biofilm formation, including the crucial function of antibiotic production is under the control of transcription factors from the GBL binding family [10,13–16]. GBLs are small diffusible molecules that control the quorum sensing process, which links the cell density to downstream gene regulation in *Streptomyces* genus [17–19].

Structural breakthrough in the GBL binding family of transcriptional factors has been achieved only for the protein CprB from *Streptomyces coelicolor* [15,16]. The structure confirmed the presence of the two domains, one associated with DNA-binding and the other responsible for signal detection through the formation of ligand–protein complex. The DNA binding domain is constituted of a HTH motif and is highly conserved among this family of proteins (Fig. 1a). By virtue of sequence and structural similarity it has been classified into the generic superfamily of tetracycline transcriptional regulator (TetR) family of repressors [20]. The TetR family of proteins consists of several proteins most of which bind to antibiotics and serve as regulators of the efflux pump pathway. Very recently the structure of CprB along with a consensus DNA (CS sequence; Fig. 1b) was solved [13,21]. The structure revealed that CprB binds to this semi-palindromic sequence as a dimer of dimer. This binding event induces a pendulum like motion that results in reorganization of various interactions across the individual dimeric interfaces. Comparison of the X-ray structure revealed that the DNA

Abbreviations: GBL, γ-butyrolactone; 2-AP, 2-aminopurine; HTH, helix-turn-helix; CS, consensus sequence; OPB, operator of CprB; MEM, Maximum Entropy Method; IRF, instrument response function; EMSA, electrophoretic mobility shift assay.

* Corresponding authors.
E-mail addresses: gk@tifr.res.in (G. Krishnamoorthy), ruchi@chem.iitb.ac.in (R. Anand).

http://dx.doi.org/10.1016/j.bbagen.2015.08.008
0304-4165/

Fig. 1. (a) Amino acid sequence conservation in the DNA-binding motif: Sequence alignment of N-terminal DNA binding domain of the GBL binding family of transcriptional repressors from *Streptomyces*, with completely conserved residues and residues conserved in four to five proteins colored maroon and orange, respectively; (b) DNA sequences known to be bound by CprB: The conserved bases of the OPB and CS sequences are shown in blue; (c) 2-AP incorporated sequences: OPB and CS sequences with 2-AP (indicated as A* in red), incorporated at the 5th, 12th and the 23rd positions.

bound form of CprB was structurally most similar to the multidrug efflux regulator QacR protein from the antibiotic resistant strain *Staphylococcus aureus* [22], thereby indicating the possibility of an analogous role in *S. coelicolor*.

In a recent study, CprB was also shown to bind a host of promoter sequences in *S. coelicolor* with varying affinity [13]. Most of these sequences influence both GBL and antibiotic production in the organism. Furthermore, based on the consensus sequence the potential cognate DNA of CprB was identified to be a 27 base pair sequence (OPB sequence, Fig. 1b) located upstream of its own gene. The study revealed that CprB, like many other TetR family proteins, apart from controlling several other genes is also likely to be autoregulatory in nature [13]. Since CprB binds to several DNA sequences an understanding of its selectivity and mode of binding to the cognate sequence is of paramount importance. Structural information of the complex with cognate OPB sequence and the other sequences that CprB differentially binds remain unavailable. This is due to the difficulty in obtaining crystals as well as a good resolution data for the protein–DNA complexes. The need for such comparison however draws attention to the alternate parameters that also confer the necessary information pertaining to the binding studies.

In this context, information regarding both site specific and overall mode of binding can be obtained by studying the motional dynamics of a non-invasive fluorescent probe introduced at specific positions across the length of the DNA sequence, in the absence and presence of the protein. 2-Aminopurine (2-AP) is a commonly used fluorophore that serves as a molecular marker in such studies [23–29]. It is an adenine analogue that forms Watson–Crick base pair with thymine and a wobble base pair with cytosine [30–32]. 2-AP has been used successfully in numerous instances to reveal various aspects of DNA–protein interactions like base flipping in methyltransferases [33,34], recognition of DNA mismatch [35], local melting by DNA polymerases [36–38], and DNA unwinding by helicases [39]. This is primarily achieved by analyzing the fluorescence intensities, lifetimes, anisotropy and local dynamics of 2-AP within the DNA by utilizing its environment-sensitivity. The motional dynamics information when combined with existing structural data can be a powerful approach to create a structural footprint for a plethora of sequences.

In the present study we analyze the extent of perturbation at three base positions, 5th, 12th and 23rd, of both the consensus (CS_5, CS_12 and CS_23) and cognate (OPB_5, OPB_12 and OPB_23) sequences upon protein binding (Fig. 1c). This was achieved by substituting 2-AP in place of the conserved adenine at these positions. The fluorescence lifetimes and anisotropy decay parameters of 2-AP were measured for the DNA and DNA in complex with CprB. Together, the information generated from 2-AP dynamics at the three conserved base positions and the available crystal structure were utilized to understand the altered motional dynamics of DNA in the presence of the protein and generate a structural footprint of DNA binding for the cognate OPB sequence.

2. Material and methods

2.1. Purification of proteins

The clone of the native protein CprB in pET26b(+) expression vector was kindly provided to us by Ryo Natsume (Japan Biological Informatics Consortium (JBIC), Tokyo, Japan). The procedures for cloning, expression and purification have been previously reported [40]. The proteins were finally desalted into buffer containing 50 mM sodium phosphate pH 7 and 180 mM NaCl and used for fluorescence studies.

2.2. DNA synthesis

The oligonucleotides with 2-AP modification and their complementary sequences were synthesized in using a MerMade 4 automated synthesizer (Bioautomation, Plano, Texas, USA). All strands were synthesized at 1 μmole scale with appropriate Controlled Pore Glass beads (Proligo Reagents, Hamburg, Germany) used as 3′ solid support. 2-Aminopurine phosphoramidite (Glen Research Corporation, Virginia, USA) was added for the incorporation of 2-AP in a sequence. The DNA sequences synthesized were purified by denaturing PAGE (20%, 7 M urea) using standard protocols. All the DNA sequences with the 2-AP modification have been characterized by MALDI-TOF-MS (Supporting information, Table S1).

The oligonucleotides were quantified by employing spectrophotometer (GE, GeneQuant 1300, WI, USA) at 260 nm. The complementary strands of the modified (2-AP incorporated) DNA, were taken in 20% excess, so as to ensure complete annealing of the fluorophore incorporated DNA. The DNA sequences were annealed in the presence of 1 X annealing buffer (5 mM Tris–HCl, pH 7.5, 15 mM NaCl, 0.1 mM EDTA). The mixture was subjected to a temperature of 95 °C for 5 min by placing in a water bath which was then allowed to cool slowly to room temperature. The samples were stored at −20 °C.

2.3. Electrophoretic mobility shift assay

The binding affinity studies of CprB to the CS and OPB sequences were carried out with the help of 5′-end radio labeled oligonucleotides.

Protein concentrations from 6 μM to 90 nM (in buffer 50 mM sodium phosphate pH 7, 180 mM NaCl) obtained by 2-fold serial dilution, were incubated with approximately 1 nM of radiolabeled and annealed DNA. The protocol that was followed for the assay has been reported previously [13].

2.4. Time-resolved fluorescence

Time resolved fluorescence decay and anisotropy decay measurements were performed using a Rhodamine 6G dye laser that generates pulses of 1 ps width. The dye laser was pumped by a passively modelocked frequency doubled Nd:YAG laser (Vanguard, Spectra Physics). The oligonucleotide samples containing 2-AP (with or without the protein) were excited at 310 nm which was the second harmonic output of angle-tuned KDP crystal. The curves for fluorescence decay were obtained from a time correlated single-photon counting setup which was coupled to a microchannel plate photomultiplier (model 2809U, Hamamatsu Corp.). The instrument response function (IRF) was obtained at 310 nm using a very dilute colloidal suspension of dried non-dairy coffee whitener. The half-width of the IRF was ~40 ps. The fluorescence emission for the excited samples was collected through a 345 nm cutoff filter followed by a monochromator at 370 nm with a collection bandwidth of 3 nm. The number of counts in the peak channel was ~10,000 for most cases except where the decay was very fast, for which the counts were kept at ~25,000. The fluorescence emission for lifetime measurements was monitored at 54.7° (magic angle) to avoid contribution from anisotropy decay. The emission was collected at directions, parallel and perpendicular to that of the incident polarized light, for the time-resolved anisotropy measurements. For more details see elsewhere [27,28,35,41].

Since one of the fluorescence lifetimes was <40 ps (see 'Results and discussion') the decay kinetics were also recorded by using a Streak Camera set-up (Model SC-10, Optronics, Kehl, Germany). Half width of the IRF was ~5 ps. In the Streak Camera experiments only one ultrafast lifetime was obtained (τ_1). This is may have been due to the instrument response time of Streak Camera being longer than that of the down-conversion set-up.

The samples consisted of 10 μM oligonucleotides, with and without the protein at 40 μM concentration. The complex was incubated at room temperature for 10 min before data collection. The buffer consisted of 50 mM Phosphate and 180 mM NaCl, pH 7.

2.5. Data analysis

The analysis of the data of fluorescence decay for the lifetime measurements were performed using FluoFit Pro Version 4.4 (PicoQuant) by a non-linear least-squares iterative reconvolution method based on the Levenberg–Marquardt algorithm [42] and expressed as a sum of exponentials with the equation:

$$I(t) = \Sigma \alpha_i \exp(-t/\tau_i) \tag{1}$$

where α_i represents the amplitude of the i*th* component associated with fluorescence lifetime τ_i such that $\Sigma\alpha_i = 1$. $\Sigma\alpha_i\ \tau_i$ gives us the mean lifetime τ_m of the system which gives knowledge about the average fluorescence yield of the system. The support plane analysis was performed to determine the confidence intervals for each parameter [43].

2.5.1. Analysis of fluorescence anisotropy decay kinetics

The time-resolved anisotropy decay curves were derived from the experimentally obtained $I_{\parallel}(t)$ and $I_{\perp}(t)$ with the equation:

$$r(t) = \frac{I_{\parallel}(t) - G(\lambda) I_{\perp}(t)}{I_{\parallel}(t) + 2G(\lambda) I_{\perp}(t)} \tag{2}$$

where $r(t)$ is the time dependent anisotropy, $I_{\parallel}(t)$ and $I_{\perp}(t)$ are the fluorescence intensity collected with the emission polarizer at 0° (parallel) and 90° (perpendicular), with respect to excitation polarizer, respectively, and $G(\lambda)$ is the geometry factor at the wavelength of emission λ. The value of $G(\lambda)$ for the optics for measuring emission was calculated independently using 50 μM solution of 2-AP.

$$I_{\parallel}(t) = I(t)[1 + 2r(t)]/3 \tag{3}$$

$$I_{\perp}(t) = I(t)[1 - r(t)]/3 \tag{4}$$

The fluorescence anisotropy decays were fitted using FluoFit into a bi-exponential model as follows:

$$r(t) = r_0[\beta_1 \exp(-t/\phi_1) + \beta_2 \exp(-t/\phi_2)] \tag{5}$$

where r_0 is the anisotropy in the absence of any rotational diffusion and β_i is the amplitude associated with the *i*th rotational correlation times ϕ_i, such that $\sum\beta_i = 1$. This model assumes that the sample contains a population having uniform motional dynamics properties with each species associated with two rotational correlation times [35]. In general, fluorescence anisotropy decay kinetics can be analyzed by one of the following two models [44]: (A) Multiple populations of the fluorophore (revealed by multiple exponentials in fluorescence intensity decay) have the same motional dynamics and (B) Multiple populations of fluorophore with each population having their own motional dynamics. Model B has been used in situations where more than one population is encountered [45–47]. In such situations anisotropy decay kinetics has complex shapes such as 'dip-and-rise' which has been fitted by model B. In contrast, multiple exponentials arising from microstates of macromolecules have been assumed to have similar motional dynamics (Model A) since multiple exponentials can have their origin in several ways including excited state reactions etc. Hence in the present work we have analyzed our results based on model A. Further justification for the use of this model is given later.

The r_0 value was estimated by a separate experiment with a sample in 70% glycerol, which was 0.31. The goodness of fits was assessed from the reduced χ^2 values (1.2–1.7) as well as from the randomness of the residuals. The support plane analysis was again performed to determine the confidence intervals for each parameter. For more details see elsewhere [27,28,35,41,43]. The results of the anisotropy decay analysis have been analyzed in terms of the change in S^2 for the probe, before and after the binding of protein, where S is the generalized order parameter [48]. S provides a measure of the restriction in the local motion of the probe and is given by the following equation [25,49]:

$$S^2 = \beta_2/(\beta_1 + \beta_2) \tag{6}$$

2.6. Maximum entropy method of analysis

The distribution of 2-AP conformers with different lifetimes, in the duplex DNA as well as in DNA–protein complex was also analyzed by the Maximum Entropy Method (MEM) of analysis [50,51]. It is a model free approach which initially assumes the fluorescence decay as a distribution of discrete lifetime values that are equally spaced in the $\log(\tau)$ space within a range which is determined by the nature of the particular fluorophore. A range of 10 ps to 20 ns was given for 2-AP. The method initially gives equal amplitude to all the lifetime values and with each iteration the distribution changes towards obtaining minimization of χ^2 and maximization of the Shannon–Jaynes entropy function given by:

$$S = \Sigma \alpha_i \log \alpha_i \tag{8}$$

where α_i represents the amplitude of the i*th* lifetime.

3. Results and discussion

3.1. DNA binding studies of CprB with CS and OPB DNA

The first sequence identified to bind CprB was the CS sequence [21] and subsequently this sequence was used to find the OPB sequence [13]. While CS sequence had been selectively pulled out from a random pool of chemically synthesized DNA sequences, the OPB sequence appears in the *S. coelicolor* genome and is therefore more biologically significant. The overall binding strength of CprB to the two sequences was estimated from electrophoretic mobility shift assays (Fig. 2). For the CS and OPB sequences an average of three data points was used to estimate the dissociation constant.

CprB exhibited similar levels of affinity for both the sequences (K_d for CS 1.26 ± 0.63 μM; K_d for OPB, 1.53 ± 0.96 μM). This could be attributed to the fact that both the sequences exhibit 52% sequence similarity and hence the binding to the two sequences CS and OPB is possibly arising from certain specific interactions among the conserved bases. However, this is not always the case as in an earlier study CprB had been shown to exhibit gradation in binding affinity with sequences of the TetR family of proteins to which the protein bears similarity in the DNA binding motif [13]. The assays performed here only give the overall binding affinity of the DNA–protein system and does not shed any light on the mode of binding or site specific dynamics which is an important aspect that needs investigation. To confirm whether the substitution of adenine by 2-AP had caused a change in the affinity of the protein towards the sequences, EMSA was also performed with all the modified DNA sequences (Fig. S1). The modified DNA sequences exhibited affinities similar to the original sequence.

3.2. Fluorescence intensity decay kinetics of 2-AP in OPB and CS DNA sequences

Free 2-AP has a quantum yield of 0.68 in an aqueous solution (pH 7) [52] and a single lifetime of ~11 ns [53]. However, when the fluorophore is incorporated in an oligonucleotide sequence, a very significant reduction in its quantum yield is often observed as a result of various interactions of 2-AP with its neighboring bases [23,24]. The degree of quenching of 2-AP is highly susceptible to perturbations in the local environment of the fluorophore in the sequence [23,24,53,54]. Moreover, 2-AP when present within a DNA displays a multi-exponential decay representative of a heterogeneous population of fluorophores with time constants ranging from ~10 ps to ~10 ns [23,24,35,41]. The population heterogeneity has been explained in terms of the existence of an array of microstates, with different degrees of DNA stacking.

The shortest lifetime component that is representative of base-pair formation in a double stranded DNA, is also related to the stronger stacking interactions of 2-AP with the neighboring bases. However, there could be other models such as excited state electron transfer to nearby guanines [23,24,54–56] resulting in multiple exponentials.

Fluorescence decay kinetics for all the DNA sequences were best represented as a sum of four components with distinct lifetimes (1). The decay was also analyzed by the MEM that presents an impartial representation of the four lifetimes.

As seen in Fig. 3, four distinguishable peaks corresponding to the lifetimes obtained from the discrete analysis (Table 1) indicate the validity of four lifetimes inferred from MEM. Decay parameters listed in Table 1 show that the shortest lifetime component (τ_1) is the major component in all the cases. Both the CS and OPB duplex DNA exhibit a very short value of mean lifetime τ_m due to the large amplitude (α_1) of the shortest lifetime species. Compared to the τ_m of single stranded DNA (Supporting information, Table S2), 2-AP in duplex DNA shows significant decrease in the value of τ_m except in the case of CS_23. The decrease is due to (i) the enhancement of stacking interaction brought about in the duplex DNA due to base pairing as compared to the less ordered single stranded DNA [23,24,55,56] and/or (ii) electron transfer to bases (mainly guanine) either adjacent to 2-AP or in the opposite strand [55]. Significantly less reduction, observed on going from single stranded to double stranded CS_23 (which does not have any guanine either adjacent or in the opposite strand), is a clear indicator that the very short lifetime in other duplex DNA is primarily due to electron transfer quenching by nearby guanine. Addition of CprB caused significant changes in the fluorescence decay kinetics of 2-AP in all the DNA sequences. The main changes are the increase in the value of τ_1, decrease in the value of α_1 and increase in the amplitude (α_4) of the longest lifetime component (τ_4) that result in the significant increase in the value of τ_m in all the cases (Table 1). The increase in the mean lifetime was a combined result of an overall increase in all the individual lifetimes as well as a shift of the population of fluorophores. For example, a comparison across the OPB DNA shows an increase in mean lifetime by 5 and 3.6 times at the 5th and 23rd positions as compared to a slightly smaller increase by 2.5 at the 12th position. This increase in the mean lifetime can be due to local perturbation caused at specific positions due to binding by CprB.

3.3. Motional dynamics from fluorescence anisotropy decay

Unlike fluorescence lifetime which is modulated by a variety of causes, fluorescence anisotropy kinetics is dominantly controlled by motional dynamics of the fluorophore and hence could be a robust read-out of protein binding to DNA. Fluorescence anisotropy decays of 2-AP in the DNA and DNA–protein complexes represented in Fig. 4 show position dependent motional dynamics of 2-AP in both the free OPB and CS sequences.

The decays were fitted satisfactorily to a sum of two exponentials. The shorter correlation time (ϕ_1), represents the local motion of the 2-AP with respect to the DNA backbone while the longer one (ϕ_2) represents the combined effect of both segmental motion within the DNA strand as well as the or the overall tumbling motion of whole strand. Most importantly, from the analysis of the anisotropy decay, the spatial

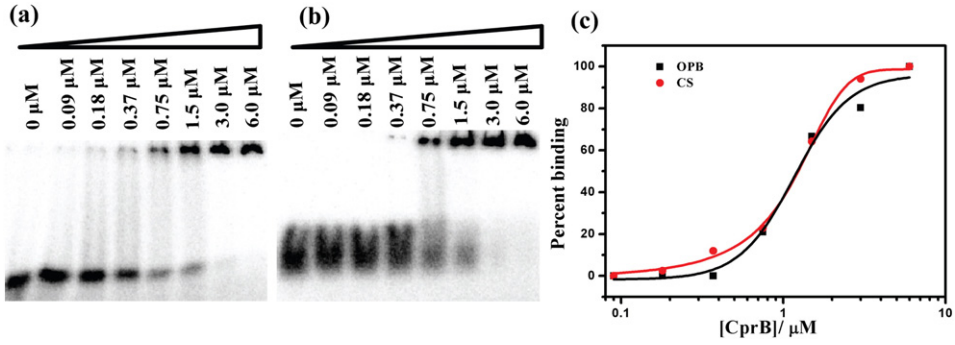

Fig. 2. DNA binding affinity of CprB: Electrophoretic mobility shift assay of CprB with (a) CS and (b) OPB DNA with increasing protein concentration as denoted in the figures. (c) Percentage binding of CprB to the DNA sequences CS (red circles) and OPB (black squares).

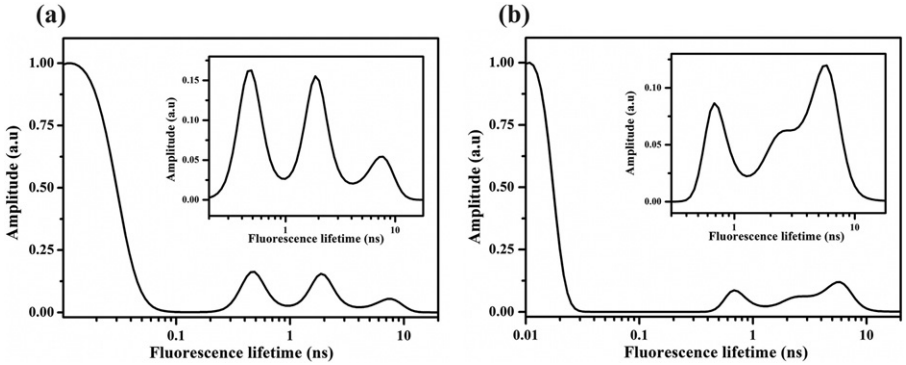

Fig. 3. Fluorescence lifetime distribution of 2-AP: The distribution of the fluorescence lifetime of 2-AP in OPB_5 (a) and its complex with CprB (b), as obtained by MEM analysis with the distribution of the lower population species, shown inset in expanded form.

restriction felt by the probe within the DNA can be comprehended from the value of S^2 as seen in Table 2.

Several observations could be made on the position dependence of motional dynamics of 2-AP in the two DNA sequences studied: (i) local motion represented by ϕ_1, is significantly slower in CS DNA when compared to OPB DNA and (ii) 2-AP at the CS_23 position has significantly slower dynamics when compared to other positions in the CS DNA. Position-dependence of motional dynamics of 2-AP in duplex DNA and especially the unusual slow dynamics of 2-AP in between two thymine bases (as in CS_23) have been observed in earlier studies [25,49].

Although the position-dependence of local dynamics (ϕ_1) could come from the variation in the level of stacking interactions of 2-AP with the adjoining bases, depolarization resulting from stacking-induced mixing of electronic states of 2-AP with that of adjacent bases could not be ruled out [23,57].

Complex formation with CprB has significant effects on the correlation times ϕ_1 and ϕ_2. As expected, complex formation resulted in retardation of the tumbling motion of the 2-AP represented by the larger value of ϕ_2 due to the increase in the overall size of the complex as compared to the free DNA. Furthermore there was an enhancement in the local dynamics of the 2-AP represented by the shortened values of ϕ_1 in all the complexes even though there was a decrease in the space available for such movement as indicated by the increase in the value of S^2 (Table 2). The increase in the value of the generalized order parameter S is associated with the restriction imposed on the free movement of 2-AP in the sequence as a result of interactions with the protein. Although shortening of ϕ_1 after binding of CprB may seem counter-intuitive, such behavior had been observed in other systems also [26,58]. These changes may again have their origin in the either or both the factors mentioned above.

Comparison of the CprB binding induced increase in the value of S^2 indicated that the level of restriction imposed by the protein varies across both the DNA sequences (Fig. 5). It was observed that in the CS series of DNA, there was a large increase in S^2 by approximately 0.55 for the 2-AP at the 5th position and also an increase of 0.43 for the 23rd position. The 12th position showed the minimum increase of 0.32. It is evident from the figures that the protein poses greater restrictions to the movement of the 2-AP, at either end of the oligomer than in the center. For the OPB DNA series as well there is a clear indication of restriction imposed by complex formation to the movement of 2-AP.

The value of S^2 increases by 0.35, 0.23 and 0.40 for OPB_5, OPB_12 and OPB_23 respectively. Comparison of the results of anisotropy decay analysis between the two sequences reveals a remarkable similarity in the manner the bases at the equivalent positions in the DNA are restricted by the protein (Fig. 5). Even though the amount of restriction at the equivalent positions varies, there is high resemblance in the trend by which the restriction is imposed at the positions. The dynamics in both the DNA sequences seem to be largely affected by protein binding towards the end positions and much less in the central position. However, it was observed that the CS sequence exhibited an overall larger restriction in dynamics on complex formation than the OPB sequence. The reason could be attributed to the difference in the inherent nature of the two sequences. The OPB sequence is comparatively more GC rich than the CS sequence and probably this is the reason it exhibits higher degree of base stacking even in the absence of the protein. Protein binding therefore seems to induce a greater degree of structure in the CS sequence as is evident from the greater overall restriction observed for this sequence as compared to the OPB sequence.

In order to validate the observations from the site-specific studies performed with the CprB-binding sequences, a control sequence was also analyzed. The control sequence consisted of the probe incorporated in a non-interacting position created by a poly-A extension at the 3′ end of the OPB sequence (Control sequence, Ct: 5′-AGGCAGGCGGCACGGT CTGTTGAGTTCAAAAAA*A-3′; A* represents 2-AP). The successful binding of the overall sequence was evident from the increase in value of the longer correlation time ϕ_2, which indicates slower global motion of the probe due to increase in its bulkiness. As observed from the generalized order parameter, the effect on the restriction to local motion of the probe in the control sequence was however negligible ($\Delta S^2 \sim 0.03$, Table 2, Supporting information Fig. S2). This reveals the specific nature of the CprB binding preferentially to the signature sequence and confirms that the changes in ΔS^2 seen earlier are due to specific interaction of the probe with CprB.

Quenching of fluorescence of 2-AP by acrylamide could also provide a site-specific map of binding of CprB to the DNA sequences. Bimolecular quenching constant k_Q estimated from Stern-Volmer plots associated with quenching by acrylamide [44] were found to be in the range of 10^{10} M^{-1} s^{-1} for all the positions in both the DNA and in the range of 10^9 M^{-1} s^{-1} for the CprB–DNA complexes (data not shown). This decrease is insensitive to any particular position along the length of the DNA sequence and only provides a global signature of protein binding. Therefore, as mentioned earlier, we believe fluorescence anisotropy as a more reliable technique to study site specific changes.

3.4. Structural correspondence of CprB–CS complex to the observed alteration in base dynamics

In order to get an in-depth understanding of how the motional dynamics at a specific position corresponds to the local structure, we analyzed the relationship between the changes in base motional restriction upon protein binding at each modified position with the interactions observed in the X-ray structure.

From the structure of CprB with a truncated CS sequence, it was observed that the adenine at the 5th position interacts more extensively with the protein than the adenine moieties present at the 12th and 23rd position (Fig. 6a). The region around the 5th base is well anchored into the major groove of the DNA making extensive interactions with residues residing in the recognition helix α3. The phosphate backbone

Table 1
Time resolved fluorescence decay parameters for 2-AP in duplex DNA and in DNA–protein complex with confidence intervals for all parameters calculated using the support plane method.

Sample	Fluorescence lifetime (τ_i, ns), amplitude (α_i)								Mean lifetime τ_m (ns)
	τ_1	α_1	τ_2	α_2	τ_3	α_3	τ_4	α_4	
CS_5	0.021 (−0.019 + 0.002)	0.98 (−0.05 + 0.04)	0.22 (−0.04 + 0.05)	0.012 (−0.001 + 0.026)	1.09 (−0.16 + 0.55)	0.005 (−0.001 + 0.002)	5.32 (−0.11 + 1.77)	0.003 (−0.001 + 0.001)	0.042
CS_5_CprB	0.029 (−0.028 + 0.004)	0.93 (−0.16 + 0.70)	0.29 (−0.18 + 0.19)	0.027 (−0.009 + 0.040)	1.93 (−0.60 + 1.89)	0.017 (−0.005 + 0.011)	6.16 (−0.53 + 9.43)	0.028 (−0.011 + 0.005)	0.24
CS_12	0.020 (−0.019 + 0.010)	0.96 (−0.60 + 0.24)	0.21 (−0.05 + 0.082)	0.022 (−0.004 + 0.006)	0.90 (−0.38 + 0.38)	0.009 (−0.002 + 0.006)	5.26 (−0.99 + 2.45)	0.004 (−0.001 + 0.001)	0.053
CS_12_CprB	0.026 (−0.004 + 0.006)	0.93 (−0.32 + 0.08)	0.56 (−0.08 + 0.09)	0.036 (−0.006 + 0.006)	3.72 (−2.73 + 0.87)	0.028 (−0.006 + 0.004)	9.90 (−4.15 + 19.2)	0.010 (−0.006 + 0.009)	0.24
CS_23	0.057 (−0.029 + 0.028)	0.39 (−0.39 + 0.23)	0.34 (−0.09 + 0.06)	0.49 (−0.18 + 0.04)	0.65 (−0.17 + 0.47)	0.12 (−0.11 + 0.01)	4.93 (−1.10 + 13.3)	0.004 (−0.002 + 0.001)	0.29
CS_23_CprB	0.047 (−0.021 + 0.032)	0.48 (−0.24 + 0.24)	0.33 (−0.05 + 0.06)	0.44 (−0.09 + 0.05)	0.96 (−0.24 + 1.19)	0.058 (−0.041 + 0.048)	5.44 (−0.45 + 1.38)	0.020 (−0.006 + 0.002)	0.33
OPB_5	0.024 (−0.022 + 0.004)	0.93 (−0.19 + 0.65)	0.31 (−0.13 + 0.21)	0.033 (−0.007 + 0.016)	1.77 (−0.24 + 0.58)	0.028 (0.008 + 0.012)	6.90 (−0.71 + 1.54)	0.010 (−0.003 + 0.005)	0.15
OPB_5_CprB	0.031 (−0.010 + 0.007)	0.77 (−0.34 + 0.16)	0.32 (−0.16 + 0.23)	0.064 (−0.016 + 0.037)	2.28 (−0.48 + 0.52)	0.087 (−0.019 + 0.017)	6.50 (−0.64 + 0.80)	0.079 (−0.023 + 0.017)	0.76
OPB_12	0.023 (−0.009 + 0.004)	0.98 (−0.37 + 0.39)	0.35 (−0.31 + 5.87)	0.005 (−0.005 + 0.036)	1.37 (−1.25 + 4.52)	0.008 (−0.007 + 0.003)	5.40 (−1.15 + 16.6)	0.005 (−0.004 + 0.002)	0.062
OPB_12_CprB	0.026 (−0.005 + 0.005)	0.96 (−0.31 + 0.51)	0.33 (−0.14 + 0.23)	0.015 (−0.004 + 0.008)	2.15 (−0.58 + 1.02)	0.014 (−0.004 + 0.005)	6.18 (−0.69 + 2.59)	0.015 (−0.006 + 0.003)	0.15
OPB_23	0.037 (−0.091 + 0.006)	0.84 (−0.21 + 0.51)	0.61 (−0.50 + 0.05)	0.079 (−0.049 + 0.064)	1.95 (−0.10 + 1.22)	0.051 (−0.011 + 0.051)	5.74 (−0.60 + 1.71)	0.028 (−0.016 + 0.016)	0.34
OPB_23_CprB	0.044 (−0.041 + 0.031)	0.62 (−0.30 + 0.31)	0.46 (−0.44 + 0.25)	0.10 (−0.05 + 0.12)	2.09 (−0.39 + 0.92)	0.13 (−0.05 + 0.08)	6.20 (−0.38 + 1.10)	0.140 (−0.03 + 0.03)	1.21

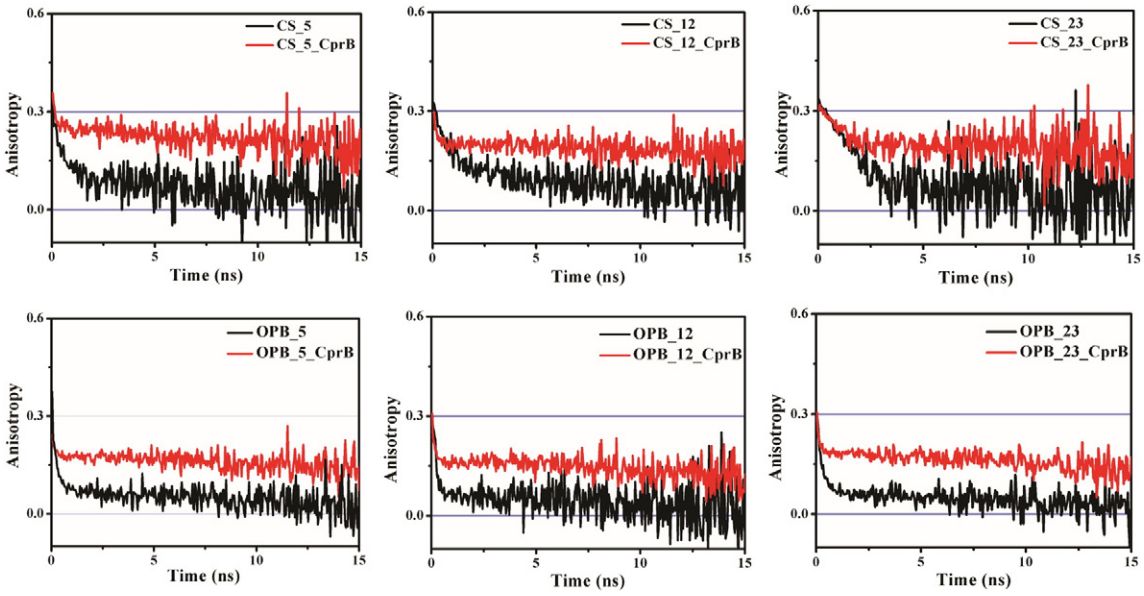

Fig. 4. The fluorescence anisotropy decay traces of 2-AP in the duplex DNA (black) and their complexes with CprB (red).

of the adjacent bases anchors this adenine group such that it makes several (Fig. 6b) hydrophobic interactions with conserved residues F48, A45 and G44 both with the purine ring as well as the deoxyribose moiety. There is also a hydrogen bonding interaction between the backbone phosphate group (joining the adenine to the neighboring thymine) and T42. Based on structural data it can be concluded that the cumulative effect of these interactions should result in restricted motion upon DNA binding at the 5th position. The large dynamic restriction observed on the 2-AP substituted at this position corroborates these conclusions. Similarly, from the analysis of the structure it was predicted that the 12th position should have the least restriction as this region of the DNA is relatively far from the protein. It was observed that the adenine base at the 12th position (Fig. 6c) showed hydrophobic interactions of its purine ring with the long aliphatic side chain of the K43 of α3. It is

Table 2
Fluorescence anisotropy decay parameters for 2-AP in free duplex DNA and in DNA–protein complex with confidence intervals for all parameters calculated using the support plane method.[a]

Sample	Rotational correlation time (ϕ_i, ns), amplitude (β_i)				S^2
	ϕ_1	β_1	ϕ_2	β_2	
CS_5	0.44 (−0.06 + 0.06)	0.76 (−0.05 + 0.04)	12.4 (−4.4 + 10.5)	0.24 (−0.04 + 0.05)	0.24
CS_5_CprB	0.26 (−0.12 + 0.31)	0.21 (−0.05 + 0.05)	>20.0	0.79 (−0.02 + 0.02)	0.79
CS_12	0.61 (−0.09 + 0.10)	0.64 (−0.04 + 0.04)	>20.0	0.36 (−0.04 + 0.04)	0.36
CS_12_CprB	0.13 (−0.03 + 0.03)	0.32 (−0.03 + 0.03)	>20.0	0.68 (−0.01 + 0.01)	0.68
CS_23	2.15 (−0.06 + 0.13)	0.79 (−0.01 + 0.01)	>20.0	0.21 (−0.01 + 0.01)	0.21
CS_23_CprB	1.05 (−0.20 + 0.25)	0.36 (−0.04 + 0.04)	>20.0	0.64 (−0.04 + 0.04)	0.64
OPB_5	0.17 (−0.02 + 0.02)	0.71 (−0.03 + 0.03)	15.9 (−2.7 + 3.7)	0.29 (−0.01 + 0.02)	0.29
OPB_5_CprB	0.06 (−0.02 + 0.02)	0.36 (−0.05 + 0.06)	>20.0	0.64 (−0.01 + 0.01)	0.64
OPB_12	0.21 (−0.03 + 0.03)	0.67 (−0.04 + 0.04)	>20.0	0.33 (−0.02 + 0.02)	0.33
OPB_12_CprB	0.080 (−0.01 + 0.02)	0.44 (−0.03 + 0.03)	>20.0	0.56 (−0.01 + 0.01)	0.56
OPB_23	0.15 (−0.02 + 0.02)	0.75 (−0.02 + 0.02)	10.9 (−1.8 + 2.3)	0.25 (−0.01 + 0.01)	0.25
OPB_23_CprB	0.07 (−0.01 + 0.02)	0.35 (−0.04 + 0.04)	>20.0	0.65 (−0.01 + 0.01)	0.65
CS_5_F48A	0.10 (−0.06 + 0.07)	0.25 (−0.04 + 0.04)	>20.0	0.75 (−0.01 + 0.01)	0.75
CS_12_K43A	0.11 (−0.03 + 0.04)	0.37 (−0.04 + 0.04)	>20.0	0.63 (−0.01 + 0.01)	0.63
Ct	0.36 (−0.05 + 0.05)	0.47 (−0.02 + 0.02)	10.1 (−1.0 + 1.2)	0.53 (−0.02 + 0.02)	0.53
Ct_CprB	0.32 (−0.05 + 0.06)	0.44 (−0.03 + 0.03)	>20.0	0.56 (−0.02 + 0.02)	0.56

[a] The lower limit in the estimation of ϕ_2 is caused by the finite lifetime window available for monitoring the decay of fluorescence anisotropy. Ct is a control sequence where 2-AP is far away from the protein binding site.

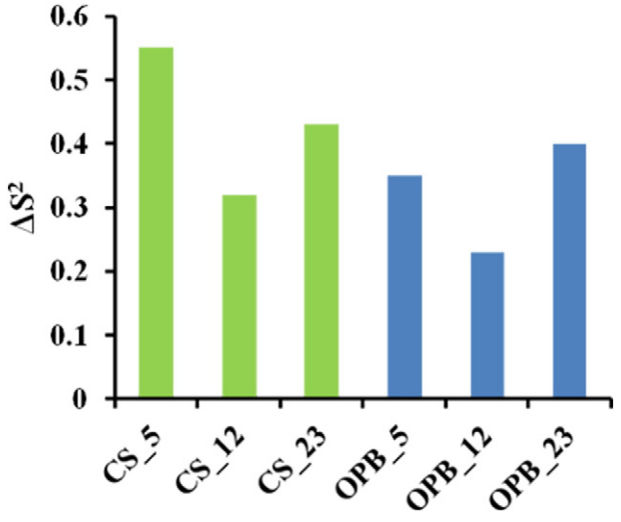

Fig. 5. Comparison of the increase in the value of S^2 for local motion of 2-AP in CS (green) and OPB (blue) sequences.

noted that among the three positions studied, the change in the value of S^2 is least for the 12th position thereby implying the lowest restriction at this position upon protein binding. This is not surprising as the 12th position (as apparent from the structure) lies in the region of the DNA which acts like a bridge between the recognition elements and exhibits least interaction with the protein. The 23rd base position however shows a similarity to the 5th position in terms of the change in S^2. This was expected as this position also lies in the region of the recognition sequence, which induced fits into the helix-turn-helix motif of CprB (Fig. 6d). The overall dynamic restriction profile of the DNA–protein system consisting of greater restriction at the end positions as compared to the central position therefore corresponded well with the environment of the bases as observed from the structure. Hence, this analysis highlights the fact that the motional dynamics along the length of the DNA, possess an underlying structural footprint. This form of analysis can be employed to predict the structural orientation of the DNA with respect to the protein. Furthermore, the correspondence between the site-specific changes in the generalized order parameter and the known structural features of the CS-DNA-CprB complex gives us credibility in using the model A (see Experimental section) for analysis of fluorescence anisotropy decay kinetics.

Since X-ray crystallography data is not available for the biologically relevant OPB sequence we utilized the comparison of the motional dynamics pattern of CS with the OPB sequence to generate a structural footprint for the cognate OPB sequence. The analysis shows that both the sequences exhibit a similar dynamic signature, with the 5th and the 23rd position exhibiting a higher overall change in the generalized order parameter as compared to the central 12th position. Therefore, it can be concluded that the overall global structure of the OPB sequence is most likely similar to that of CS. However, it appears that the CS sequence has an overall character of being more dynamically restrained by the protein as compared to the OPB sequence. The restraint is enhanced in the 5th and 23rd positions as these positions are in close proximity of the surrounding protein. However, a close look at the values observed at the individual positions revealed that unlike the CS sequence where the motion at the 5th position is most restrained in the OPB sequence it is the 23rd position which exhibits the maximum constrain in motion. Thus the order of restriction in local dynamics is 5th > 23rd > 12th in the CS sequence is now changed to 23rd > 5th > 12th for the OPB sequence. This is most likely because

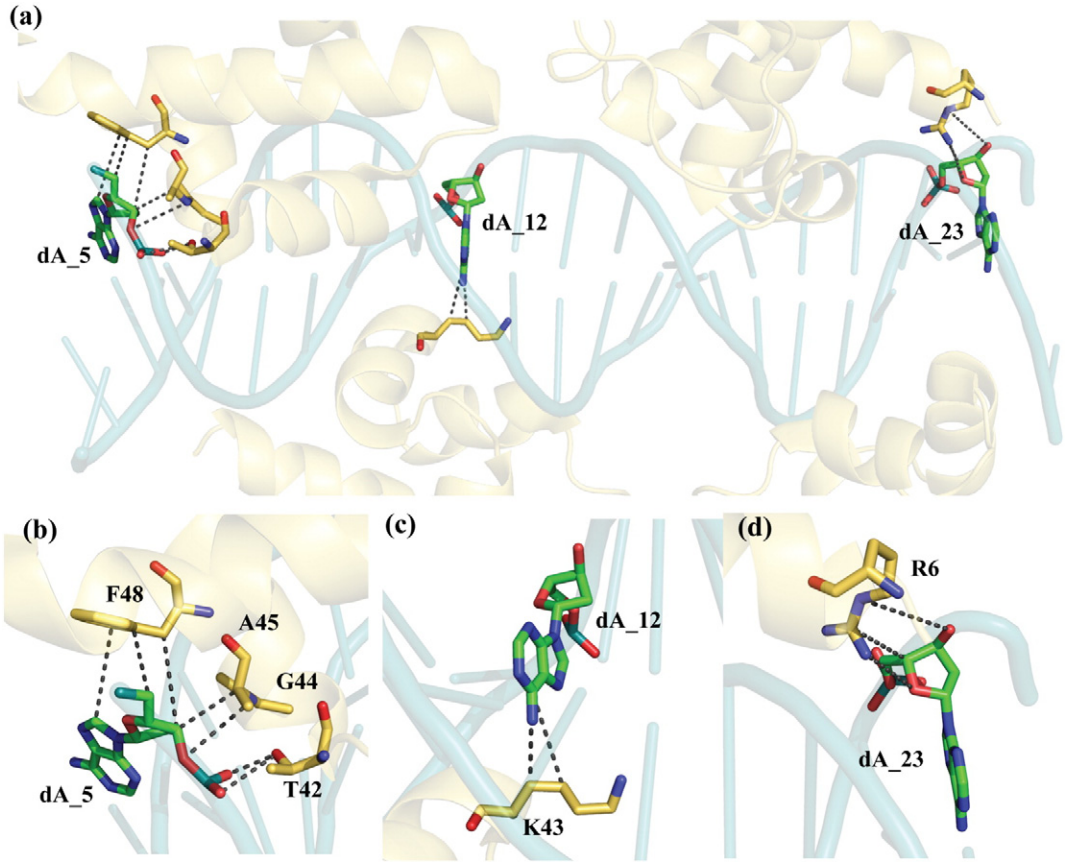

Fig. 6. Protein–DNA interactions as observed in CprB–CS DNA complex: (a) The CprB–CS DNA complex (PDB ID: 4PXI) showing the adenine bases (dA) that have been replaced by 2-AP. (b), (c) and (d) show the interactions of adenine bases at the 5th, 12th and 23rd positions of CS sequence, with CprB.

both the CS and the OPB sequences exhibit a small degree of difference in the recognition elements that are presented to the protein. For example as compared to CS, OPB sequence is more GC rich. Though there exists a high degree of similarity in the general mode of binding, fine differences could arise from certain preferred interactions of one DNA over the other, by virtue of the dissimilarities in their sequences. Hence, it is noteworthy that the dynamic study can reveal even the fine tuning of interactions by the protein on two quite similar sequences that is otherwise difficult to extract. The results are very significant in the case of proteins such as CprB that are known to bind a multitude of sequences. Though obtaining the crystal structure of complexes with every cognate DNA of the proteins is not always feasible, it is however possible to delineate the mode of binding for all the cases using 2AP as a site-specific probe.

3.5. Dynamics study with CprB mutants

To analyze the influence of disrupting interactions at the CprB–DNA interface, conserved residues F48 and K43 whose side chains are involved in contact with the bases were mutated to alanine residue. Both F48 and K43 make hydrophobic interactions with the adenine bases at the 5th and 12th positions respectively. Fluorescence anisotropy results show that in the absence of these individual interactions binding of CS_5 and CS_12 to mutants F48A and K43A resulted in a marginal decrease in the S^2 by 0.04 and 0.05 respectively (Table 2, Supporting Information Fig. S3). The decrease indicates the role of these residues in the restriction of the corresponding bases in the sequence.

However, since the decrease in the value of S^2 due to the mutations are not drastic it asserts the fact that single point removal of a side chain does not affect the local and overall binding of the protein to the DNA by a large extent and the effect is most likely cumulative. These results are in accord with gel shift experiments performed on an earlier report where single mutations did not exhibit reduced binding affinity, whereas double mutants showed a marked reduction in binding affinity [13]. Our attempts to perform experiments with the double mutants resulted in noisy un-interpretable data mostly because the double mutants were intrinsically unstable and could not be obtained in concentrations required for a proper dynamic study.

4. Conclusions

In this study we investigated the alteration in the dynamics of 2-AP incorporated at certain selected positions in two DNA sequences, CS and OPB, on binding of the protein CprB. The aim was to illustrate how the method can be successfully used to study the mode of binding of the protein to various regions of the DNA site-specifically. In the study, 2-AP in all double stranded DNA exhibited a very short lifetime that was probably caused mainly from electron transfer to bases either adjacent to 2-AP or in the opposite strand. The influence of the neighboring bases was evident from the comparison of the contribution of the shortest lifetime species to the mean lifetime with the 2-AP of CS_23 standing out due to the absence of guanine as an immediate neighbor or in the opposite strand.

In the absence of the structure of CprB with the biologically relevant OPB sequence, a combination of structural and motional dynamics information was employed to generate a structural footprint. In terms of the restriction in the local motion, the protein binding clearly causes an increase in the motional restriction of bases at all positions within the signature binding sequence. The DNA restriction parameters exhibited a similar overall binding pattern, with a larger restriction at the 5th and the 23rd position as compared to the middle 12th position. The results have been accounted for from the interactions observed in the structure of CprB in complex with the consensus sequence. However, due to the differences in base composition of the two sequences local differences in restriction at individual positions were observed. The analysis suggested that unlike in the CS sequence where the base at the 5th position is strongly anchored, in the OPB sequence it is the base at the 23rd position that is preferably stabilized. Therefore, this approach apart from providing global structural correspondence can also give information about fine details of individual interactions. Hence, we can use it to deduce a structural footprint for individual protein–DNA interactions for proteins that bind to a multitude of sequences (such as the pleiotropic regulator CprB).

Acknowledgments

The authors thank Ryo Natsume for the CprB plasmid in pET26b(+) and N. Periasamy for providing the software used in the analysis of time-resolved fluorescence data. The authors are also thankful to A. Datta for his suggestions and Pradeepkumar P. I. for providing the automated DNA synthesizer for the synthesis of the oligonucleotides used in the experiments. G. Krishnamoorthy is a recipient of J. C. Bose National Research Fellowship from the Government of India. The authors also thank CSIR, New Delhi for the fellowship of A. Biswas and IIT Bombay, Mumbai and TIFR, Mumbai for providing all the necessary facilities. This work was also supported by DBT (BT/PRI3766/BRB/10/785/2010) and DST (SR/S/BB-53/2010).

Appendix A. Supplementary data

Supplementary data to this article can be found online at http://dx.doi.org/10.1016/j.bbagen.2015.08.008.

References

[1] D. Beckett, Regulated assembly of transcription factors and control of transcription initiation, J. Mol. Biol. 314 (2001) 335–352.
[2] C.W. Muller, Transcription factors: global and detailed views, Curr. Opin. Struct. Biol. 11 (2001) 26–32.
[3] S. Tan, T.J. Richmond, Eukaryotic transcription factors, Curr. Opin. Struct. Biol. 8 (1998) 41–48.
[4] C.O. Pabo, R.T. Sauer, Transcription factors: structural families and principles of DNA recognition, Annu. Rev. Biochem. 61 (1992) 1053–1095.
[5] S.V. Razin, V.V. Borunova, O.G. Maksimenko, O.L. Kantidze, Cys2His2 zinc finger protein family: classification, functions, and major members, Biochem. Mosc. 77 (2012) 217–226.
[6] H.J. Thiesen, C. Bach, DNA recognition of C2H2 zinc-finger proteins, Ann. N. Y. Acad. Sci. 684 (1993) 246–249.
[7] L. Aravind, V. Anantharaman, S. Balaji, M.M. Babu, L.M. Iyer, The many faces of the helix-turn-helix domain: Transcription regulation and beyond, FEMS Microbiol. Rev. 29 (2005) 231–262.
[8] R.G. Brennan, B.W. Matthews, The helix-turn-helix DNA binding motif, J. Biol. Chem. 264 (1989) 1903–1906.
[9] R. Wintjens, M. Rooman, Structural classification of HTH DNA-binding domains and protein–DNA interaction modes, J. Mol. Biol. 262 (1996) 294–313.
[10] M. Folcher, H. Gaillard, L.T. Nguyen, K.T. Nguyen, P. Lacroix, N. Bamas-Jacques, M. Rinkel, C.J. Thompson, Pleiotropic functions of a *Streptomyces pristinaespiralis* autoregulator receptor in development, antibiotic biosynthesis, and expression of a superoxide dismutase, J. Biol. Chem. 276 (2001) 44297–44306.
[11] D. D'Alia, D. Eggle, K. Nieselt, W.S. Hu, R. Breitling, E. Takano, Deletion of the signalling molecule synthase ScbA has pleiotropic effects on secondary metabolite biosynthesis, morphological differentiation and primary metabolism in *Streptomyces coelicolor* A3(2), Microb. Biotechnol. 4 (2010) 239–251.
[12] E. Bateman, M. Kivie, Autoregulation of eukaryotic transcription factors, Progress in Nucleic Acid Research and Molecular Biology, vol. 60, Academic Press 1998, pp. 133–168.
[13] H. Bhukya, R. Bhujbalrao, A. Bitra, R. Anand, Structural and functional basis of transcriptional regulation by TetR family protein CprB from *S. coelicolor* A3(2), Nucleic Acids Res. 42 (2014) 10122–10133.
[14] S. Kitani, Y. Yamada, T. Nihira, Gene replacement analysis of the butyrolactone autoregulator receptor (FarA) reveals that FarA acts as a novel regulator in secondary metabolism of *Streptomyces lavendulae* FRI-5, J. Bacteriol. 183 (2001) 4357–4363.
[15] R. Natsume, Y. Ohnishi, T. Senda, S. Horinouchi, Crystal structure of a gamma-butyrolactone autoregulator receptor protein in *Streptomyces coelicolor* A3(2), J. Mol. Biol. 336 (2004) 409–419.
[16] R. Natsume, R. Takeshita, M. Sugiyama, Y. Ohnishi, T. Senda, S. Horinouchi, Crystallization of CprB, an autoregulator-receptor protein from *Streptomyces coelicolor* A3(2), Acta Crystallogr., Sect. D: Biol. Crystallogr. 59 (2003) 2313–2315.
[17] E. Takano, Gamma-butyrolactones: *Streptomyces* signalling molecules regulating antibiotic production and differentiation, Curr. Opin. Microbiol. 9 (2006) 287–294.
[18] N.H. Hsiao, S. Nakayama, M.E. Merlo, M. de Vries, R. Bunet, S. Kitani, T. Nihira, E. Takano, Analysis of two additional signaling molecules in *Streptomyces coelicolor*

and the development of a butyrolactone-specific reporter system, Chem. Biol. 16 (2009) 951–960.
[19] E. Takano, T. Nihira, Y. Hara, J.J. Jones, C.J. Gershater, Y. Yamada, M. Bibb, Purification and structural determination of SCB1, a gamma-butyrolactone that elicits antibiotic production in *Streptomyces coelicolor* A3(2), J. Biol. Chem. 275 (2000) 11010–11016.
[20] J.L. Ramos, M. Martinez-Bueno, A.J. Molina-Henares, W. Teran, K. Watanabe, X. Zhang, M. Gallegos, R. Brennan, R. Tobes, The TetR family of transcriptional repressors, Microbiol. Mol. Biol. Rev. 69 (2005) 326–356.
[21] H. Onaka, S. Horinouchi, DNA-binding activity of the A-factor receptor protein and its recognition DNA sequences, Mol. Microbiol. 24 (1997) 991–1000.
[22] M.A. Schumacher, M.C. Miller, S. Grkovic, M.H. Brown, R.A. Skurray, R.G. Brennan, Structural basis for cooperative DNA binding by two dimers of the multidrug-binding protein QacR, EMBO J. 21 (2002) 1210–1218.
[23] J.M. Jean, K.B. Hall, 2-Aminopurine electronic structure and fluorescence properties in DNA, Biochemistry 41 (2002) 13152–13161.
[24] E.L. Rachofsky, R. Osman, J.B.A. Ross, Probing structure and dynamics of DNA with 2-aminopurine: effects of local environment on fluorescence, Biochemistry 40 (2001) 946–956.
[25] S.V. Avilov, E. Piemont, V. Shvadchak, H. de Rocquigny, Y. Mely, Probing dynamics of HIV-1 nucleocapsid protein/target hexanucleotide complexes by 2-aminopurine, Nucleic Acids Res. 36 (2008) 885–896.
[26] J. Godet, N. Ramalanjaona, K.K. Sharma, L. Richert, H. de Rocquigny, J.L. Darlix, G. Duportail, Y. Mely, Specific implications of the HIV-1 nucleocapsid zinc fingers in the annealing of the primer binding site complementary sequences during the obligatory plus strand transfer, Nucleic Acids Res. 39 (2011) 6633–6645.
[27] T. Goel, T. Mukherjee, B.J. Rao, G. Krishnamoorthy, Fluorescence dynamics of double- and single-stranded DNA bound to histone and micellar surfaces, J. Phys. Chem. B 114 (2010) 8986–8993.
[28] T.S. Singh, B.J. Rao, G. Krishnamoorthy, GTP binding leads to narrowing of the conformer population while preserving the structure of the RNA aptamer: a site-specific time-resolved fluorescence dynamics study, Biochemistry 51 (2012) 9260–9269.
[29] S. Bharill, P. Sarkar, J.D. Ballin, I. Gryczynski, G.M. Wilson, Z. Gryczynski, Fluorescence intensity decays of 2-aminopurine solutions: lifetime distribution approach, Anal. Biochem. 377 (2008) 141–149.
[30] L.C. Sowers, G.V. Fazakerley, R. Eritja, B.E. Kaplan, M.F. Goodman, Base pairing and mutagenesis: observation of a protonated base pair between 2-aminopurine and cytosine in an oligonucleotide by proton NMR, Proc. Natl. Acad. Sci. 83 (1986) 5434–5438.
[31] P.A. Fagan, C. Fabrega, R. Eritja, M.F. Goodman, D.E. Wemmer, NMR study of the conformation of the 2-aminopurine: cytosine mismatch in DNA, Biochemistry 35 (1996) 4026–4033.
[32] L.C. Sowers, Y. Boulard, G.V. Fazakerley, Multiple structures for the 2-aminopurine-cytosine mispair, Biochemistry 39 (2000) 7613–7620.
[33] B.W. Allan, N.O. Reich, Targeted base stacking disruption by the EcoRI DNA methyltransferase, Biochemistry 35 (1996) 14757–14762.
[34] B. Holz, E. Weinhold, S. Klimasauskas, S. Serva, 2-Aminopurine as a fluorescent probe for DNA base flipping by methyltransferases, Nucleic Acids Res. 26 (1998) 1076–1083.
[35] N. Nag, B.J. Rao, G. Krishnamoorthy, Altered dynamics of DNA bases adjacent to a mismatch: a cue for mismatch recognition by MutS, J. Mol. Biol. 374 (2007) 39–53.
[36] R.A. Hochstrasser, T.E. Carver, L.C. Sowers, D.P. Millar, Melting of a DNA helix terminus within the active site of a DNA polymerase, Biochemistry 33 (1994) 11971–11979.
[37] S.S. Mandal, E. Fidalgo da Silva, L.J. Reha-Krantz, Using 2-aminopurine fluorescence to detect base unstacking in the template strand during nucleotide incorporation by the bacteriophage T4 DNA polymerase, Biochemistry 41 (2002) 4399–4406.
[38] U. Subuddhi, M. Hogg, L.J. Reha-Krantz, Use of 2-aminopurine fluorescence to study the role of the beta hairpin in the proofreading pathway catalyzed by the phage T4 and RB69 DNA polymerases, Biochemistry 47 (2008) 6130–6137.
[39] K.D. Raney, L.C. Sowers, D.P. Millar, S.J. Benkovic, A fluorescence-based assay for monitoring helicase activity, Proc. Natl. Acad. Sci. 91 (1994) 6644–6648.
[40] A. Biswas, R.K. Swarnkar, B. Hussain, S.K. Sahoo, P.I. Pradeepkumar, G.N. Patwari, R. Anand, Fluorescence quenching studies of gamma-butyrolactone binding protein (CprB) from *Streptomyces coelicolor* A3(2), J. Phys. Chem. B 118 (2014) 10035–10042.
[41] T. Ramreddy, M. Kombrabail, G. Krishnamoorthy, B.J. Rao, Site-specific dynamics in TAT triplex DNA as revealed by time-domain fluorescence of 2-aminopurine, J. Phys. Chem. B 113 (2009) 6840–6846.
[42] P.R. Bevington, Data Reduction and Error Analysis for the Physical Sciences, McGraw Hill, Inc., New York, 1969.
[43] M. Straume, S.J. Frasier-Cadoret, M.L. Johnson, Least-squares analysis of fluorescence data, in: J.R. Lakowicz (Ed.) Topics in Fluorescence Spectroscopy, vol. 2, Plenum Press, New York 1991, pp. 177–240.
[44] J.R. Lakowicz, Principles of Fluorescence Spectroscopy, Kluwer Academic/Plenum Publishers, New York, 2006.
[45] G. Krishnamoorthy, A. Srivastava, Cell type and spatial location dependence of cytoplasmic viscosity measured by time-resolved fluorescence microscopy, Arch. Biochem. Biophys. 340 (1997) 159–167.
[46] A. Jha, J.B. Udgaonkar, G. Krishnamoorthy, Characterization of the heterogeneity and specificity of interpolypeptide interactions in amyloid protofibrils by measurement of site-specific fluorescence anisotropy decay kinetics, J. Mol. Biol. 393 (2009) 735–752.
[47] A. Jha, S. Narayan, J.B. Udgaonkar, G. Krishnamoorthy, Solvent-induced tuning of internal structure in a protein amyloid protofibril, Biophys. J. 103 (2012) 797–806.
[48] G. Lipari, A. Szabo, Effect of librational motion on fluorescence depolarization and nuclear magnetic resonance relaxation in macromolecules and membranes, Biophys. J. 30 (1980) 489–506.
[49] P. Rai, T.D. Cole, E. Thompson, D.P. Millar, S. Linn, Steady state and time resolved fluorescence studies indicate an unusual conformation of 2-aminopurine within ATAT and TATA duplex DNA sequences, Nucleic Acids Res. 31 (2003) 2323–2332.
[50] J.C. Brochon, Maximum entropy method of data analysis in time-resolved spectroscopy, Methods Enzymol. 240 (1994) 262–311.
[51] R. Swaminathan, N. Periasamy, Analysis of fluorescence decay by the maximum entropy method: Influence of noise and analysis parameters on the width of the distribution of lifetimes, Proc. Indian Acad. Sci. Chem. Sci. 108 (1996) 39–49.
[52] D.C. Ward, E. Reich, L. Stryer, Fluorescence studies of nucleotides and polynucleotides. I. Formycin, 2-aminopurine riboside, 2,6-diaminopurine riboside, and their derivatives, J. Biol. Chem. 244 (1969) 1228–1237.
[53] C.R. Guest, R.A. Hochstrasser, L.C. Sowers, D.P. Millar, Dynamics of mismatched base pairs in DNA, Biochemistry 30 (1991) 3271–3279.
[54] A. Holmen, B. Norden, B. Albinsson, Electronic transition moments of 2-aminopurine, J. Am. Chem. Soc. 119 (1997) 3114–3121.
[55] S.O. Kelley, J.K. Barton, Electron transfer between bases in double helical DNA, Science 283 (1999) 375–381.
[56] C. Wan, T. Fiebig, O. Schiemann, J.K. Barton, A.H. Zewail, Femtosecond direct observation of charge transfer between bases in DNA, Proc. Natl. Acad. Sci. 97 (2000) 14052–14055.
[57] K.B. Hall, D.J. Williams, Dynamics of the IRE RNA hairpin loop probed by 2-aminopurine fluorescence and stochastic dynamics simulations, RNA 10 (2004) 34–47.
[58] M. Bailey, P. Hagmar, D.P. Millar, B.E. Davidson, G. Tong, J. Haralambidis, W.H. Sawyer, Interaction between the *Escherichia coli* regulatory protein TyrR and DNA: a fluorescence footprinting study, Biochemistry 34 (1995) 15802–15812.